Polyhedron 31 (2012) 649–656

Contents lists available at SciVerse ScienceDirect

Polyhedron

journal homepage: www.elsevier.com/locate/poly

Oxido-pincer complexes of copper(II) – An EXAFS and EPR study of mono- and binuclear $[(pydotH_2)CuCl_2]_n$ (n = 1 or 2)

Axel Klein [a,*], Katharina Butsch [a,1], Sait Elmas [a], Christian Biewer [a], Dominikus Heift [a,2], Sara Nitsche [a], Irene Schlipf [b], Helmut Bertagnolli [b]

[a] Universität zu Köln, Department für Chemie, Institut für Anorganische Chemie, Greinstrasse 6, D 50939 Köln, Germany
[b] Universität Stuttgart, Institut für Physikalische Chemie, Pfaffenwaldring 55, D-70569 Stuttgart, Germany

ARTICLE INFO

Article history:
Received 11 January 2011
Accepted 19 October 2011
Available online 28 October 2011

Keywords:
Oxido-pincer ligand (O,N,O ligand)
Copper(II)
EPR spectroscopy
EXAFS
Coordination geometry

ABSTRACT

The oxido-pincer ligand $pydotH_2$ (2,6-bis(1-hydroxy-1-*o*-tolyl-ethyl-η^2O,O′)pyridine) forms two different Cu^{II} containing complexes when prepared from anhydrous $CuCl_2$. A combination of EPR spectroscopy and EXAFS allowed to structurally characterise the light-green dimer of the formula $[(pydotH_2)CuCl(\mu\text{-}Cl)_2ClCu(pydotH_2)]$ and the penta-coordinate olive-green monomer $[(pydotH_2)CuCl_2]$. The molecular entities imply that the ligand remains protonated upon coordination. When dissolved in DMF both compounds form monomeric species $[(pydotH_2)CuCl_2(DMF)]$ which could be characterised in detail by EPR, UV–Vis/NIR spectroscopy and electrochemical measurements. The assignments were supported by comparison with Cu^{II} complexes of the related ligands 2,6-bis(hydroxymethyl)pyridine ($pydimH_2$) and 2,6-bis(1-hydroxy-1-methyl)pyridine ($pydipH_2$).

1. Introduction

Lying on the edge between the d block metals and the main group elements, copper is one of the most studied transition metals. One can trace back the high interest in this metal and the vast number of applications to mainly two fundamental properties. First, the element can easily shuttle between the two oxidation states Cu^{I} and Cu^{II}, which explains e.g. the frequent use of copper in redox-active metalloenzymes [1–4]. The reason for this is that, although Cu^{I} with a d^{10} configuration is the intrinsically more stable form, suitable ligand surrounding or even solvation can markedly stabilise Cu^{II} (d^9). This is combined with the second aspect, which is the high flexibility of both copper oxidation states in coordination number and geometry. While for Cu^{I} in unrestrained and non biological surrounding the major coordination geometry is tetrahedral, the d^9 configuration of Cu^{II} leads to the well-known Jahn-Teller distortion (or related distortions) and as a consequence numerous coordination numbers (4–6) and geometries (square planar, square pyramidal, tetragonally elongated or compressed octahedral, trigonal bipyramidal) were observed for Cu^{II} complexes [4–8]. As a consequence, when preparing new Cu^{II} complexes, prediction of the geometry and composition of the products is difficult and hindered by the paramagnetic character of Cu^{II} complexes disabling rapid structure elucidation by NMR spectroscopy. Frequently, this problem has been overcome by ligand design. E.g., the proper design of multidentate ligands allows to predict (design) the coordination geometry, provided the binding between the ligands donor atoms and the metal is strong [3,5,6,9–11].

From the vast group of multidentate ligands, the so called O,N,O oxido pincer ligands (Scheme 1) provide a scaffold to form Cu^{II} complexes which is interesting for several reasons. Firstly, although the oxido donor function might be varied to a large extend as depicted in Scheme 1, a relatively weak bonding of the pendant (hard) oxido donor functions to late (soft) transition metals as Cu^{II} can be expected. Secondly, these pincer ligands, which can additionally be substituted in various positions, prefer a meridional binding.

Of special interest in this respect are the ligands based on pyridine-2,6-dimethanol ($pydimH_2$; Scheme 1) since they can bind in their protonated or deprotonated form and thus provide an interesting acid–base chemistry (including potential catalytic applications) [12–15], as well as a variety of different coordination possibilities. Fully or partly deprotonated $pydimH^-$ or $pydim^{2-}$ ligands were found to form oligomeric complexes as e.g., $[Cu_2(pydimH)_2(pydimH_2)_2]^{2+}$ [16–18], $[Cu_2(\eta^2,\mu\text{-}pydimH)_2(\eta^3\text{-}pydimH_2)_2]^{2+}$, $[Cu(pydimH_2)(pydimH)]^{+}$ [17] or clusters such as $[Cu_3(O_2CMe)_2(pydim)_2(MeOH)]$ and $[Cu_4(O_2CMe)_2(pydimH)_4]^{2+}$ [19], and $[Cu_4(NO_3)_2(pydimH)_4(H_2O)(MeOH)]$ [20]. The latter are interesting magnetic materials. Even in the fully protonated form,

* Corresponding author. Tel.: +49 221 4704006; fax: +49 221 4705193.
E-mail address: axel.klein@uni-koeln.de (A. Klein).
[1] Present address: Stanford University, Department of Chemistry, Stack Lab 333 N–S Axis Stauffer 2 107, Stanford, CA 94305-5080, United States.
[2] Present address: ETH Hönggerberg, Laboratorium für Anorganische Chemie Wolfgang-Pauli-Str. 10, HCI-H114 8093 Zürich, Switzerland.

0277-5387/$ - see front matter © 2011 Elsevier Ltd. All rights reserved.
doi:10.1016/j.poly.2011.10.023

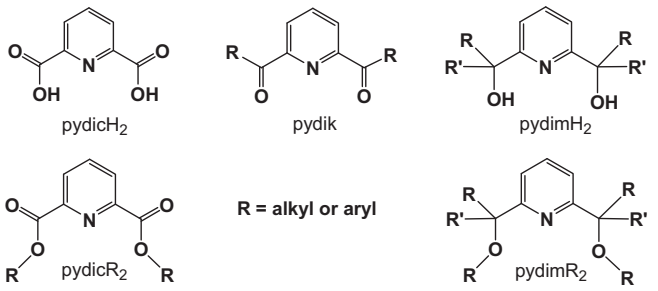

Scheme 1. Various types of oxido pincer ligands providing a O,N,O donor set ($pydicH_2$ = pyridine-2,6-dicarboxylic acid; pydik = pyridine-2,6-diketone; $pydimH_2$ = pyridine-2,6-dimethanol.

the combination of $pydimH_2$ and Cu^{II} can lead to a number of different complexes, depending on the $Cu^{II}/pydimH_2$ ratio and additional coligands. The homoleptic complex $[Cu(pydim)_2]^{2+}$ has been reported with a number of counter anions such as Cl^-, ClO_4^- [17], NO_3^- [20], propionate [21], saccharinate (1,1-dioxo-1,2-benzo[d]isothiazol-3-one-2-yl) [22], or niflumate (2-{[3-(trifluoromethyl)phenyl]amino}nicotinate) [23]. In the presence of further tridentate ligands such as pyridine-2,6-dicarboxylate octahedral complexes were formed e.g., [($pydimH_2$)Cu(pydic)] [24].

Our group has recently reported that alternatively to the established hexa-coordinate species $[Cu(O,N,O)_2]^{2+}$ penta-coordinate Cu^{II} complexes [(O,N,O)$CuCl_2$] (O,N,O = $pydimH_2$, $pydipH_2$ or $pydotH_2$; Scheme 2) can be obtained from reactions of the ligands and $CuCl_2{\cdot}2H_2O$. Furthermore, the penta-coordinate complexes were found to undergo disproportionation reactions: $2[(O,N,O)CuCl_2] \leftrightarrows [Cu(O,N,O)_2]^{2+} + [CuCl_4]^{2-}$ in polar solvents [25].

This stands in contrast to the complexes obtained from the phenoxy type of O,N,O oxido pincer ligands for which exclusively binuclear complexes $[(O,N,O)CuCl_2]_2$ were obtained from the reaction of the ligands and $CuCl_2$. When dissolved in DMF these complexes transform into mononuclear species of the composition [(O,N,O)-$CuCl_2$(DMF)] while no disproportionation was observed [26].

Since copper complexes with oxido-pincer ligands are of various interest e.g., as models for superoxide dismutases [27], as Lewis acid catalysts [14,15] or as potential non-steroidal anti-inflammatory drugs [28] the control over the nuclearity of corresponding species in the solid and in solution is crucial.

Herein we report on a detailed study on the reaction products obtained from the chiral ligand $pydotH_2$ (Scheme 2) with anhydrous $CuCl_2$. The two isolated products as well as species observed in solution were examined by a combination of EPR, UV–Vis/NIR spectroscopy, electrochemical measurements and EXAFS. Assignments were further supported by comparison with related complexes of the O,N,O ligands with established molecular structures [25].

2. Experimental

2.1. Instrumentation

Elemental analyses were carried out using a HEKAtech CHNS EuroEA 3000 Analyzer. UV–Vis/NIR absorption spectra were measured on Varian Cary50 Scan or Shimadzu UV-3600 photo spectrometers. EPR spectra were recorded in the X band on a Bruker System ELEXSYS 500E equipped with a Bruker Variable Temperature Unit ER 4131VT. Usually, single spectra were recorded at low acquisition times with a microwave power of 10 mW (or lower) and modulation amplitudes ranging between one and four Gauss, *g* values were calibrated using a dpph sample. Spectral simulation was carried out using the WINEPR Simfonia program from Bruker. Electrochemical experiments were carried out in 0.1 M nBu_4NPF_6 solutions using a three-electrode configuration (glassy carbon electrode, Pt counter electrode, Ag/AgCl reference) and an Autolab PGSTAT30 potentiostat and function generator. The ferrocene/ferrocenium ($FeCp_2/FeCp_2^+$) couple served as internal reference.

2.2. X-ray absorption spectroscopy

The EXAFS and XANES measurements were performed at the XAS beamline at the Ångströmquelle Karlsruhe (ANKA) under ambient conditions at 20 °C. The synchrotron beam current was between 80 and 140 mA at 2.5 GeV storage ring energy. A Si(1 1 1) double crystal monochromator was used for measurements at the Cu K-edge (8979 keV). The second monochromator crystal was tilted for optimal harmonic rejection. The energy resolution for the Cu K-edge energy is estimated to be 1.0 eV. The spectra were recorded in transmission mode with ionisation chambers. The first two ionisation chambers were filled with nitrogen gas, the third one with a mixture of argon and nitrogen. The individual pressures were adjusted to optimise the signal-to-noise ratio. Energy calibration was performed with a copper metal foil. To avoid mistakes in the XANES region arising from small changes in the energy calibration between two measurements, all spectra were corrected to the theoretical edge energy of copper foil, which was measured in every scan. The solid samples were embedded in a cellulose matrix and pressed into pellets. The concentration was adjusted to yield an absorption jump of $\Delta\mu d \approx 1.3$.

The data analysis of the measured XAFS spectra was performed using program packages IFEFFIT (Athena, AUTOBK) and EXCURV98 [29–31]. Data analysis in k-space in the interval k listed in Table 1 was performed using the curved wave theory with XALPHA potentials and phase shifts and the resulting EXAFS function was weighted with k^3. The amplitude reduction factor (AFAC) was determined by fitting the reference foil and set at 0.9.

2.3. Materials and procedures

The ligands $pydimH_2$, $pydipH_2$ and $pydotH_2$ and the Cu^{II} complexes [($pydimH_2$)$CuCl_2$], [($pydipH_2$)$CuCl_2$][$CuCl_4$] and [($pydipH_2$)$_2$-Cu]Cl_2 were synthesised as previously reported [25].

[($pydimH_2$)$CuCl_2$]: Synthesised from $CuCl_2{\cdot}2H_2O$ and $pydimH_2$ and isolated as turquoise crystals. Yield: 202 mg (74%).

[($pydimH_2$)$CuCl_2$]·H_2O): (*Anal.* Calc. for $C_7H_{11}Cl_2CuNO_3$: C, 28.83; H, 3.80; N, 4.80. Found: C, 28.88; H, 3.80; N, 4.78%); Carefully ground and dried samples of [($pydimH_2$)$CuCl_2$] for EPR measurements analysed to (*Anal.* Calc. for $C_7H_9Cl_2CuNO_2$: C, 30.73; H, 3.32; N, 5.12. Found: C, 30.73; H, 3.30; N, 5.13%).

[Cu($pydipH_2$)$_2$][$CuCl_4$]: Synthesised from $CuCl_2{\cdot}2H_2O$ and $pydipH_2$ and isolated as a blue powder. Yield: 306 mg (93%). (*Anal.*

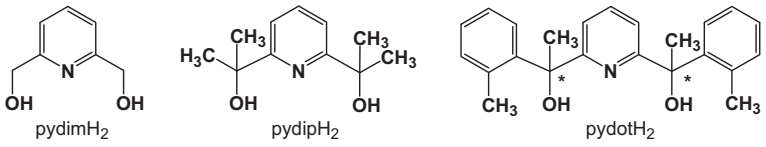

Scheme 2. O,N,O oxido pincer ligands used in this study 2,6-bis(hydroxymethyl)pyridine ($pydimH_2$), 2,6-bis(1-hydroxy-1-methyl)pyridine ($pydipH_2$) and 2,6-bis(1-hydroxy-1-*o*-tolyl-ethyl)pyridine ($pydotH_2$).

Table 1
Structural parameters of the solid Cu complexes determined from the Cu K-edge EXAFS spectra in comparison to XRD data.[a]

Compound		r (Å)	N	σ (Å)	E_0 (eV)	Fit-index k-range (Å^{-1})	XRD data (Å)[b]
[(pydimH_2)$CuCl_2$]·H_2O	Cu–N	1.92(2)	1	0.032(3)	7.654	33.28	1.929(1)
	Cu–O	2.02(2)	2	0.084(8)		3.0–14.0	1.997(2)/2.001(2)
	Cu–Cl	2.20(3)	1	0.063(6)			2.2076(7)
		2.68(3)	1	0.112(17)			2.6960(9)
	Cu···C	2.81(3)	4	0.077(12)			2.942(2)/2.845(2)/2.832(2)/2.922(2)
[(pydotH_2)$CuCl_2$]	Cu–N	1.91(2)	1	0.032(3)	6.113	30.34	
P1	Cu–O	2.03(2)	2	0.071(7)		3.0–13.0	
	Cu–Cl	2.17(2)	1	0.100(10)			
		2.61(3)	1	0.112(17)			
	Cu···C	2.77(3)	4	0.112(17)			
[(pydotH_2)CuCl(μ-Cl)$_2$ClCu(pydotH_2)]	Cu–N	1.93(2)	1	0.039(4)	6.542	31.90	
P2	Cu–O	2.01(2)	2	0.077(8)		3.0–13.5	
	Cu–Cl	2.22(2)	2	0.110(11)			
		2.55(3)	1	0.112(17)			
	Cu···C	2.86(3)	4	0.095(14)			
	Cu···Cu	3.37(3)	1	0.112(17)			
[Cu(pydipH_2)$_2$]Cl_2·H_2O	Cu–N	1.96(2)	2	0.059(6)	5.214	39.53	1.957(2)/1.958(2)
	Cu–O	2.15(2)	4	0.105(11)		3.0–13.0	2.156(2)/2.173(2)/2.179(2)/2.196(2)
	Cu···Cl	4.00(4)	2	0.092(14)			4.088(1)/4.121(1)
	Cu···C	2.86(3)	4	0.081(12)			2.882(2)/2.871(2)/2.875(2)/2.885(2)
	Cu···C	2.96(3)	4	0.087(13)			3.019(2)/3.026(2)/3.025(2)/3.039(2)

[a] Absorber-backscatterer distance r, coordination number N, Debye-Waller factor σ, shift of the threshold energy ΔE_0 and the fit-index R for the fitted k-ranges. The numbers in brackets are uncertainties in the last digits. The errors are estimated to be ±1% for distances, ±10% for Debye-Waller factors of shells with $r < 2.5$ Å and ±15% for Debye-Waller factors of shells with $r > 2.5$ Å. With respect to an unjustified expansion of the evaluation process, the coordination numbers were fixed for each evaluation and varied manually in steps of one.
[b] From ref. [25].

Calc. for $C_{22}H_{34}Cl_4Cu_2N_2O_4$: C, 40.07; H, 5.20; N, 4.25. Found: C, 40.06; H, 5.20; N, 4.23%).

[Cu(pydipH_2)$_2$]Cl_2·H_2O: Synthesised from $CuCl_2$·$2H_2O$ and pydipH_2 (2 equiv.) and isolated as a turquoise powder. Yield: 500 mg (92%). (*Anal.* Calc. for $C_{22}H_{36}Cl_2CuN_2O_5$: C, 48.66; H, 6.68; N, 5.16. Found: C, 48.65; H, 6.65; N, 5.12%).

Synthesis of dichlorido-2,6-bis(1-hydroxy-1-methyl-ethyl-η^2O,O') pyridinecopper(II) [(pydipH_2)$CuCl_2$]: An amount of 268.8 mg (2 mmol) anhydrous $CuCl_2$ and 390.5 mg (2 mmol) pydipH_2 were dissolved in 30 mL of abs. acetone (or methanol). The mixture was stirred at room temperature for 2 h, then the solvent was removed under reduced pressure and the residue recrystallised three times from acetone and pentane to afford a blue powder. Yield: 310 mg (94%). (*Anal.* Calc. for $C_{11}H_{17}Cl_2CuNO_2$: C, 40.07; H, 5.20; N, 4.25. Found: C, 40.12; H, 5.30; N, 4.26%).

Synthesis of dichloro-2,6-bis(1-hydroxy-1-o-tolyl-ethyl-η^2O,O') pyridinecopper(II) [(pydotH_2)$CuCl_2$]$_n$: An amount of 268.8 mg (2 mmol) anhydrous $CuCl_2$ and 694.4 mg (2 mmol) pydotH_2 were dissolved in 30 mL of abs. acetone. The mixture was stirred over night at room temperature, after which an orange–yellow solution has formed. Then the volume of the solvent was slowly reduced under reduced pressure to about 10 mL yielding a bright green solid (**P2**), while the solution has darkened. Evaporation of the residual solution gave an olive-green powder, which was washed with three 20 mL portions of *n*-pentane and dried (**P1**). Yield for **P1**: 770 mg (80% per Cu atom). (*Anal.* Calc. for $C_{23}H_{25}Cl_2CuNO_2$: C, 57.32; H, 5.23; N, 2.91. Found: C, 57.31; H, 5.25; N, 2.93%); Yield for **P2**: 173 mg (18% per Cu atom). (*Anal.* Calc. for $C_{23}H_{25}Cl_2CuNO_2$: C, 57.32; H, 5.23; N, 2.91. Found: C, 57.38; H, 5.28; N, 2.90%).

3. Results and discussion

3.1. Reaction of anhydrous $CuCl_2$ with pydotH_2 (2,6-bis(1-hydroxy-1-o-tolyl-ethyl)pyridine)

The reaction of anhydrous $CuCl_2$ with pydotH_2 in dry acetone (see Section 2) leads simultaneously to two different products **P1** and **P2** (Scheme 3). Upon evaporation of the yellow orange reaction solution, first a grass green product (**P2**) is precipitating and can be filtered off. When no further grass green precipitate is observed, the final olive green to brown solution is evaporated to dryness giving an olive-green solid (**P1**). Elemental analysis confirms the identical elemental composition of the two complexes and from these observations we assume that **P1** and **P2** have the same chemical composition and stand in equilibrium with each other. While **P1** is readily soluble in organic solvents as CH_2Cl_2, THF, acetone, DMF or MeCN, **P2** dissolves only very slowly in DMF or MeCN yielding olive green solutions (see absorption spectroscopy). From the different solubility we assume that the grass green product **P2** is a binuclear species, while the olive green derivative **P1** is the corresponding monomer.

P2 is assumed to be a chlorido-bridged binuclear complex with an "equatorial" coordination plane formed by the pyridine N atoms, all four chlorido ligands and the two Cu^{II} ions. This conformation is supposed from the rigidity of the O,N,O ligand, allowing only equatorial tris-chelate coordination, as has been shown for related mononuclear complexes of 3d transition metals [17,25,32], but has also been reported for various other complexes *e.g.* with dialkylpyridine-2,6-dicarboxylate (O,N,O) [33] or bis(pyridin-2-ylmethyl)amino]methyl}-2-phenolate (N_3O) ligands [34]. For Cu^{II} complexes of the ligands pydimH_2 and pydipH_2 (Scheme 2), which were closely related to pydotH_2, exclusively the **P1** forms were observed so far. This was unequivocally concluded from the high solubility in common organic solvents, the UV–Vis/NIR spectra and from XRD of [(pydimH_2)$CuCl_2$]·H_2O [25]. Also for Ni^{II}, Co^{II}, and Zn^{II} mononuclear complexes with structures similar as **P1** have been reported by us recently [25].

When reacting pydimH_2 with anhydrous $CuCl_2$ under the same conditions as pydotH_2 but in acetone or methanol solution, a green powder is obtained which analyses to [(pydimH_2)$CuCl_2$]$_n$. Although the compound is virtually insoluble, from the EPR spectrum of the isolated powder (see below) we can assign the compound to the monomer ($n = 1$). The same compound has been recently obtained from the reaction of the ligand with $CuCl_2$·$2H_2O$ in aqueous ethanol [25]. In contrast to this, the reaction of pydipH_2 with anhydrous $CuCl_2$ either in acetone or in methanol leads to a blue compound, which analysed correctly to be composed of the ligand and $CuCl_2$

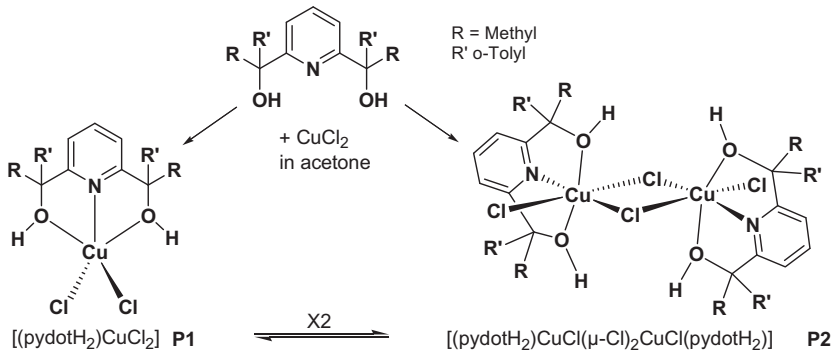

Scheme 3. Reaction of the ligand pydotH_2 with anhydrous $CuCl_2$.

in a 1:1 ratio. The EPR spectrum of the isolated powder and absorption spectroscopic investigation clearly reveals that the product is $[Cu(pydipH_2)_2][CuCl_4]$ (see below). The related compound $[Cu(pydipH_2)_2]Cl_2$ has been recently obtained from the reaction of the ligand with $CuCl_2{\cdot}2H_2O$ in a 2:1 ratio in ethanol [25], which allowed the unequivocal assignment.

In view of our previous results [25] we can summarise the results on the preparation as follows. When ligand and $CuCl_2$ are reacted in a 1:1 ratio the penta-coordinate complexes $[(O,N,O)CuCl_2]$ and/or the products of the disproportionation reaction (1) were obtained.

$$2[Cu(O,N,O)_2][CuCl_4] \leftrightarrows [(O,N,O)CuCl_2] \quad (1)$$

Since the disproportionation reaction is not very fast, for pydimH_2 exclusively the penta-coordinate complex $[(pydimH_2)CuCl_2]$ is obtained which, due to its low solubility, precipitates rapidly from the reaction mixture. For pydotH_2 a mixture of mononuclear and binuclear $[(pydotH_2)CuCl_2]_n$ ($n = 1$ or 2) is obtained, since most of the initially formed penta-coordinate species immediately precipitates from the reaction mixture in the form of the (insoluble) dimer. This rapid precipitation leaves no time for the slow disproportionation and at the end of the isolation process small amounts of the monomeric complex can be obtained by rapid work-up. For the pydipH_2 ligand the solubility of all species is high and after extended reaction time (over night) exclusively the products of the disproportionation were obtained. Shortening the reaction time markedly (2 h) allows to isolate the penta-coordinate complex $[(pydipH_2)CuCl_2]$. Additionally, the type of solvent or the water content of the reacted $CuCl_2$ varies the solubility of the products, while the rate of the disproportionation strongly depends on the solvent polarity; in CH_2Cl_2 almost no reaction is observed, even after hours, in acetone the reaction occurs perceptively already after some minutes, while in DMF the reaction is too fast to allow measurements on the penta-coordinate complexes $[(O,N,O)CuCl_2]$.

From both **P1** or **P2** we could not obtain single crystals, therefore we embarked on an XAS study of both complexes, also including the recently reported derivatives $[(pydimH_2)CuCl_2]{\cdot}H_2O$ and $[Cu(pydipH_2)_2]Cl_2{\cdot}H_2O$. The two latter have been investigated by single crystal XRD. Thus the EXAFS data can be compared with XRD data for these two compounds.

3.2. XANES and EXAFS

The Cu K-edge X-ray absorption near edge spectra (XANES) of $[(pydotH_2)CuCl_2]$ (**P1**), $[(pydotH_2)CuCl(\mu\text{-}Cl)_2ClCu(pydotH_2)]$ (**P2**), $[Cu(pydipH_2)_2]Cl_2{\cdot}H_2O$ and $[(pydimH_2)CuCl_2]{\cdot}H_2O$, were recorded (see Fig. 1). There is a scarcely observable signal at about 8976–8979 eV due to the dipole forbidden 1s → 3d transition [35], a shoulder about 8985–8989 eV and an intense resonance peak at about 8995–8998 eV. This signature can be assigned to 1s → 4p transitions and indicates that all compounds are in the oxidation state Cu^{II}. This is supported by the absence of a well-defined pre-peak at 8983–8984 eV which would be indicative for copper in the oxidation state Cu^{I} [36]. Numeric XANES results are given in Table S1 in the Supporting Information.

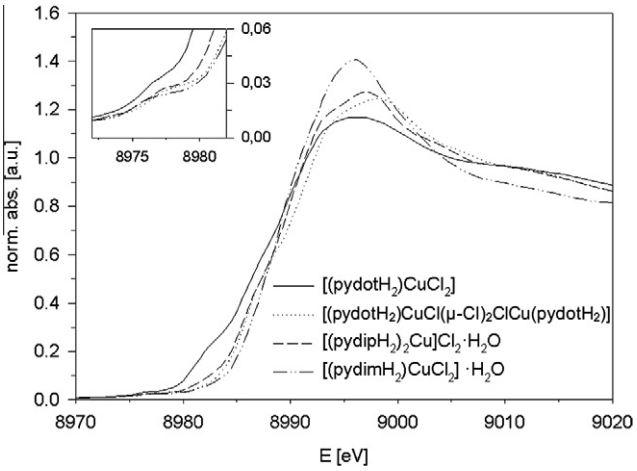

Fig. 1. Comparison of the Cu-K edge XANES spectra of $[(pydotH_2)CuCl_2]$ (solid line), $[(pydotH_2)CuCl(\mu\text{-}Cl)_2ClCu(pydotH_2)]$ (dotted line), $[(pydipH_2)_2Cu]Cl_2{\cdot}H_2O$ (dashed line) and $[(pydimH_2)CuCl_2]{\cdot}H_2O$ (dashed dotted line).

The 1s → 4p resonance transition of the Cu K-edge is substantially modified by the electronic environment such as ligand field, the chemical bonding in the initial state and by the atomic valence state [37]. Calculation of the shift of E_0 in comparison to the pure metal, ΔE_0, and the edge width ΔE_w, defined as the difference in energy between the inflection point E_0 and the main absorption maximum of the edge [38], can provide information about the structure of the studied complexes [39]. A semiquantitative correlation between the edge width and the nature and number of the surrounding atoms points to generally larger edge widths for lower coordination numbers, while ΔE_w is smaller for higher coordination polyhedra [40]. From our measurements we can state a smaller edge width ΔE_w and an increased edge shift ΔE_0 for **P1** in comparison to **P2**. The penta-coordinate complex $[(pydimH_2)CuCl_2]{\cdot}H_2O$ (structure established by XRD) exhibits values very similar to those of **P1**, which supports our assumption that **P1** is mononuclear and presumably penta-coordinate. The very different ΔE_w and ΔE_0 values for **P2** indicate marked differences to the coordination geometry of **P1**, however the values obtained for the compound $[Cu(pydipH_2)_2]Cl_2$, which has a hexa-coordinate copper core (XRD), are very much unlike those observed for **P2**. On the other hand, the Cu^{II} ion in the

complex $[Cu(pydipH_2)_2]^{2+}$ exhibits a tetragonally compressed octahedral geometry (due to the two tight *trans*-oriented Cu–N bonds), while the hexa-coordinate surrounding of the Cu^{II} ions in **P2** (Scheme 2) is completely different from the presence of the Cl ligands. Considering that not only the coordination geometry but also the electrostatic environment is changed by the formation of a chlorido-bridged binuclear complex, the variation of the edge width and the edge shift of **P1** in comparison to **P2** is reasonable.

Fig. 2 shows the EXAFS spectra of **P1** and **P2**, while the structural parameters of all investigated complexes determined by curve fitting analyses of the EXAFS spectra at the Cu K-edge are summarised and compared to XRD data in Table 1.

The fittings of the Cu K-edge EXAFS spectra (Fig. 2) of the compound **P1** and the reference complex $[(pydimH_2)CuCl_2]\cdot H_2O$ were performed using a five shell model, wherein the first two coordination shells at about 2.0 Å consist of the two coordinating oxygen atoms and one nitrogen of the pyridine-2,6-dimethanol ligands, the third and fourth shell of the chlorine backscatterers at ~2.2 and ~2.7 Å and a fifth coordination shell at ~2.8 Å of further backbone-carbon backscatterers of the chelating ligand. The fitting model for **P2** was on one hand deduced from the parameters of **P1** and an additional chlorine backscatterer at about 2.2 Å. On the other hand the structures of the related complexes $[(L)CuCl(\mu\text{-}Cl)_2ClCu(L)]$ (L = dialkylpyridine-2,6-dicarboxylate; R = Me [dmpc], Et [depc] or R = *i*Pr [dppc]) [33] were taken into account for the fitting. Based on these three structures an additional Cu-shell was added to the fit. Assuming a Cu···Cu distance at about 3.4 Å improved the fitting results significantly improved the fitting results. However, the best fit for **P2** was obtained with a coordination sphere slightly different from those of the two above mentioned complexes. The most striking difference is one long (2.55(3) Å) and two markedly shorter (2.22(2) Å) Cu–Cl distances in **P2**, in contrast to the dialkylpyridine-2,6-dicarboxylate complexes where all three Cu–Cl distances are far more similar to each other (ranging from 2.25 to 2.35 Å). Another marked difference to the dialkylpyridine-2,6-dicarboxylate complexes is that the Cu–O distances were short (about 2 Å) in **P2**, while in the latter they range between 2.35 and 2.62 Å. Importantly, in most so far structurally characterised complexes of the pyridine-2,6-dimethanol ligands (as $pydimH_2$ or $pydotH_2$) the Cu–O bonds were short [16–20,22,24,25] thus supporting our data for **P2** from EXAFS. The difference between the pyridine-2,6-dimethanol ligands and the dialkylpyridine-2,6-dicarboxylates lies not only in the different O donor atoms (OH vs. O=C or OR) but also in the OC–CNC–CO scaffold, which contains either short C=O or C–O bonds for the latter ligands, making the O–Cu–O angles markedly smaller and the Cu–O distances larger. Thus, the overall geometry of the dialkyl-2-6-dicarboxylate complexes can be described as "fused" tetragonally elongated octahedra, while **P2** resembles more a dimer of two square pyramidal configured Cu^{II} complexes. Unfortunately, from EXAFS we cannot say whether the long Cu–Cl bond is a terminal or a bridging one, presumably the latter is the case.

3.3. EPR spectroscopy

From selected samples EPR spectra were recorded on finely divided powders at ambient temperature or 110 K. Since in all cases

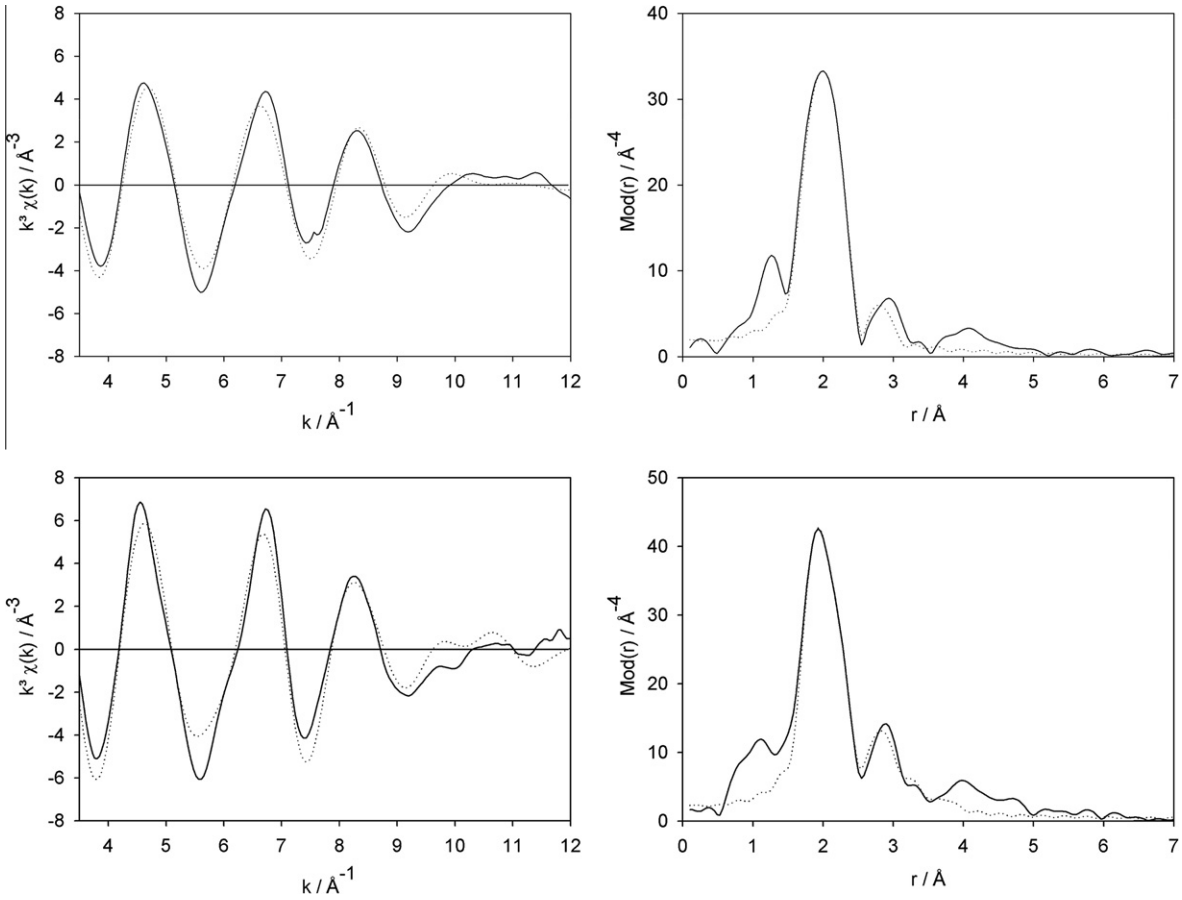

Fig. 2. Experimental (solid line) and calculated (dotted line) $k^3\chi(k)$ functions (left) and their Fourier transforms (right) of solid $[(pydotH_2)CuCl_2]$ (**P1**, top) and $[(\mu Cl_2)\{(pydotH_2)CuCl\}_2]$ (**P2**, bottom) at the Cu K-edge.

(with the exception of [(pydipH_2)$CuCl_2$]) very broad lines were observed with no hyperfine splitting (hfs), samples of **P1** and **P2** were diamagnetically diluted using $KAl(SO_4)_2$. However, also for those samples no hfs could be observed. Fig. 3 displays spectra of **P1** and **P2** underpinning their markedly different character, Table 2 lists essential EPR data of selected Cu^{II} complexes.

While **P1** shows an almost isotropic rather narrow spectrum, **P2** exhibits a complex spectral pattern and most importantly a half-field signal ($\Delta M_S = \pm 2$), which is very indicative for a binuclear complex with ferromagnetic coupling of the unpaired spins of two Cu^{II} ions in binuclear complexes resulting in an S = 1 ground state [33,34,42–46]. Interestingly, there is almost no difference between spectra of **P2** recorded at 298 K or at 110 K. The ($\Delta M_S = \pm 1$) spectrum of **P2** consists of a narrow band centred at about 2300 G and two further broad components at 2800 and 3500 G. Unfortunately, due to the lack of hfs, we were not able to simulate the spectrum of **P2** and thus could not obtain the zero-field splitting parameters D and E. This is a pity, since from these values the Cu···Cu distance could be calculated [46,47]. On the other hand

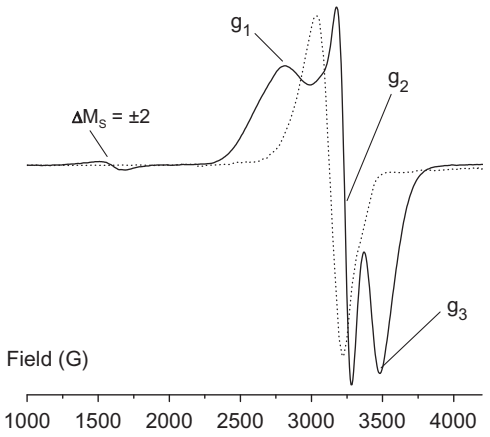

Fig. 3. X-band EPR spectra of [(pydotH_2)$CuCl_2$] (**P1**) (dotted) and [(pydotH_2)$CuCl_2$]$_2$ (**P2**) (solid line), both measured as diluted powders (1:10 with $KAl(SO_4)_2$) at 110 K.

the lack of resolved hfs is indicative for "magnetically condensed copper(II) compounds" [46]. Using the approximation of Eaton to determine D from the spectral difference of the low-field edge of the half-field signal and $h\nu/2g\beta$ [47] we obtained D ~ 340 G (E is assumed to be 0), which calculates to a Cu···Cu distance of 4.44 Å. The result shows that the assumption of purely dipolar interaction between the two unpaired electrons is not justified, in line with the assumed structure of **P2** (μ-Cl bridged Cu^{II} ions). In order to obtain more information on the coordination of the Cu^{II} ions in **P2** we wanted to compare its EPR spectrum to those of other binuclear chlorido-bridged Cu^{II} complexes (for details see Supporting Information) and thus translated the three components of the spectrum into three "observed" *g* values (Table 2). Rhombic EPR spectra were reported for [(L)CuCl(μ-Cl)$_2$ClCu(L)] (L = dialkyl-pyridine-2,6-dicarboxylate; alkyl = Et [depc] or R = *i*Pr [dppc]) both with two bridging and two terminally bound Cl ligands [33]. The depc derivative exhibits a slightly distorted octahedral geometry ($Cl_{(equatorial,short)}O_{2(axial,long)}N_{(equatorial,short)}$μ-$Cl_{2(equatorial,short)}$), around the copper atoms with a coplanar arrangement of N, Cl and Cu atoms and exhibits a g_{av} value very similar to **P2**. In contrast to this, the bulkier dppc ligand forces a butterfly-like Cu_2Cl_2 core with a strongly distorted octahedral geometry around the copper atom. Consequently, the averaged *g* value is markedly smaller. The spectrum of the complex [Cu(H_2py2th1as)(μ-Cl)]$_2$(ClO_4)$_4$ (H_2py2th1as = thiophen-2-yl)methylamino)methyl)-6-(bis((pyridin-2-yl)methyl)amino)-4-methylphenol) in the solid exhibits also a relatively low averaged *g* value and axial symmetry, which is probably due to the strong tetragonal distortion of the octahedral Cu^{II} environment ($N_{3(equatorial,short)}$μ-$Cl_{(equatorial,short)}O_{(axial,long)}$ μ-$Cl_{(axial,long)}$) [34]. Axial EPR spectra were also found for related chlorido-bridged binuclear complexes such as [Cu(HL)Cl]$_2$ (H_2L = [2-((E)-(2-hydroxyethylimino)methyl)-4-bromophenol]) [43], [Cu(apyhist)Cl]$_2^{2+}$ (apyhist = (4-imidazolyl)ethylene-2-amino-1-ethylpyridine)[42] or [$CuCl_2$(Mebta)]$_2$ (Mebta = 1-methylbenzotriazole) [44] showing five-coordinated Cu(II). Thus, the rhombic EPR spectrum of **P2** is fully in line with a dimeric structure [(pydotH_2)CuCl(μ-Cl)$_2$ClCu(pydotH_2)] with an only slightly distorted octahedral coordination environment ($O_{2(axial,short)}$ $N_{(equatorial,short)}Cl_{(terminal)}$(μ-Cl)$_2$) of the Cu^{II} ions, in agreement with the structure proposed from EXAFS. Unfortunately, the EPR data of

Table 2
Selected EPR data of Cu^{II} complexes.[a]

	g_{av}	g_1	g_2	g_3	Spectral symmetry	Molecular symmetry[b]
Mononuclear complexes						
[(pydotH_2)$CuCl_2$] (**P1**)	2.175	2.226	2.180	2.120	rhombic	SPy
[(pydimH_2)$CuCl_2$]	2.158	2.311	2.094	2.068	rhombic	SPy
[(pydipH_2)$CuCl_2$]	2.138	2.220	2.220	1.973[c]	axial compressed	TBP
[(pydipH_2)$_2$Cu]Cl_2	2.195	2.221	2.190	2.173	rhombic	OC
[(pydimH_2)Cu(pydic)][d]	2.139	2.238	2.139	2.040	rhombic	OC
[(pydotH_2)$CuCl_2$(DMF)][e]	2.194	2.353[f]	2.120	2.108	rhombic	OE
[Cu(H_2O)$_6$]$^{2+}$ [g]	2.202	2.405	2.100	2.100	axial elongated	OE
Binuclear complexes						
[(pydotH_2)$CuCl_2$]$_2$ (**P2**)[h]	2.148	2.418	2.081	1.946	rhombic	OD
[(μ-Cl)(depc)$CuCl]_2$[i]	2.147	2.21	2.12	2.11	rhombic	OD
[(μ-Cl)(dppc)$CuCl]_2$[i]	2.130	2.17	2.16	2.06	rhombic	OD
[Cu(H_2py2th1as)(μ-Cl)]$_2$(ClO_4)$_4$ [j]	2.14	2.30	2.06	2.06	axial elongated	OD

[a] All samples measured as finely divided powders at X-band frequency, at 298 K; all *g* values from spectral simulation. $g_{av} = (g_1 + g_2 + g_3)/3$; $\Delta g = g_3 - g_1$.
[b] Symmetry assignment based on EPR spectroscopy (see text), SPy = square pyramidal, TBP = trigonal bipyramidal, OC = octahedral compressed, OD = octahedral dimeric, OE = octahedral elongated.
[c] A_3 = 175 G.
[d] From Ref. [24].
[e] Measured at 110 K in glassy frozen DMF.
[f] A_1 = 107 G.
[g] From Ref. [41].
[h] *g* Values could not be obtained from simulation, *g* values are thus "observed values" as depicted in Fig. 3.
[i] From Ref. [33].
[j] Co-crystallised with 6 MeOH, from Ref. [34].

P2 does not provide unequivocal information about the position of the long Cu–Cl bond concluded from EXAFS (bridging or terminal).

Within the series of mononuclear penta-coordinate complexes $[(O,N,O)CuCl_2]$ the EPR spectra of **P1** and $[(pydimH_2)CuCl_2]$ exhibit rhombic symmetry, while $[(pydipH_2)CuCl_2]$ shows an axially compressed spectrum. The rhombic spectra are in line with the square pyramidal structure found in the crystal of $[(pydimH_2)CuCl_2]$ and assumed for the EXAFS spectra of $[(pydotH_2)CuCl_2]$. The axially compressed spectrum of $[(pydipH_2)CuCl_2]$ showing hfs to $^{35,37}Cu$ (I = 3/2, 100% nat. abundance) on the g_3 component ($g_{||}$) points to a more trigonal bipyramidal surrounding of the Cu^{II} ion [5,8,40]. The hexa-coordinate Cu^{II} complex $[(pydipH_2)_2Cu]^{2+}$ in $[(pydipH_2)_2Cu]Cl_2$ shows a rhombic spectrum very similar to the related complex $[(pydimH_2)Cu(pydic)]$ [18]. These two examples represent the small class of tetragonally compressed octahedral systems (better described as pseudo Jahn-Teller systems) [8], which contrast to the vast group of tetragonally elongated systems as $[Cu(H_2O)_6]^{2+}$ [41], which normally exhibit spectra with axial symmetry [5,8,48].

When **P1** or **P2** were dissolved in DMF, identical spectra (isotropic g = 2.193, no hfs), were obtained. At 110 K in glassy frozen solution, spectra exhibiting rhombic symmetry (g_{av} = 2.194) and hfs on the g_1 component (A_1 = 107 G) were recorded and the mononuclear species $[(pydotH_2)CuCl_2(DMF)]$ is assumed to be present in such solutions [34,42,43,45]. The rhombic character of the signal is a strong indication that the $pydotH_2$ ligand is still completely coordinated since it's rigid scaffold does not allow a "relaxed" octahedral coordination around Cu^{II} [5,48].

3.4. Absorption spectroscopy

Absorption spectra of the penta-coordinate complexes $[(O,N,O)CuCl_2]$ (including **P1**) were measured in CH_2Cl_2 or DMF solution.

Table 3
Long-wavelength absorption maxima of Cu^{II} complexes of O,N,O ligands.[a]

Compound	λ	Solvent
$[(pydotH_2)CuCl_2]$	786	CH_2Cl_2
$[(pydotH_2)CuCl_2]_2$	890	KBr
$[(pydotH_2)CuCl_2(DMF)]$	948	DMF
$[(pydipH_2)CuCl_2(DMF)]$	898	DMF
$[(pydimH_2)CuCl_2]$	775	CH_2Cl_2
$[(pydipH_2)CuCl_2]$	798	CH_2Cl_2
$[Cu(pydimH_2)_2][CuCl_4]$ [b]	892	DMF
$[Cu(pydipH_2)_2][CuCl_4]$ [b]	905	DMF

[a] Wavelength λ in nm; bands were assigned to d–d transition of the d^9 system.
[b] Further bands at 460 nm were assigned to LMCT bands originating from $[CuCl_4]^{2-}$.

The compound **P2** turned out to be insoluble in CH_2Cl_2 and solutions in DMF (in which it dissolves slowly) showed identical absorption spectra to solutions of **P1** in DMF (see Table 3). The latter spectra were assigned to the hexa-coordinate DMF complex $[(pydotH_2)CuCl_2(DMF)]$ in line with the results from EPR spectroscopy and electrochemical measurements. The corresponding hexa-coordinate solvent complex $[(pydipH_2)CuCl_2(DMF)]$ is probably observed in DMF solutions of $[(pydipH_2)CuCl_2]$, while for sparingly soluble $[(pydimH_2)CuCl_2]$ in DMF the disproportionation (see Eq. (1)) is too fast and only the disproportionation products were observed as can be inferred from the strong LMCT band of $[CuCl_4]^{2-}$ at about 460 nm. However, absorption spectra of the penta-coordinate species can be obtained in CH_2Cl_2 solution, in which the solubility of the materials is sufficient, while the disproportionation is hampered from the low polarity of the solvent. Furthermore, coordination of CH_2Cl_2 is unlikely. A spectrum of **P2** recorded from a KBr pellet shows a long-wavelength absorption maximum at rather low energy, comparable to the other hexa-coordinate complexes. Interestingly, the absorption energies for the penta-coordinate species are markedly higher than for the hexa-coordinate complexes. Obviously the loss of the relatively strong chlorido ligands, when going from the penta-coordinate to the hexa-coordinate species is not compensated by the coordination of a sixth ligand, which is further evidence for a long bridging Cu–Cl bond.

3.5. Electrochemical measurements

From selected samples cyclovoltammetric (CV) measurements were carried out using DMF as solvent and $n Bu_4NPF_6$ as electrolyte. Fig. 4 shows CVs of the hexa-coordinate $[(pydipH_2)_2Cu]Cl_2$ (left) and **P1** (right). When **P2** is dissolved in DMF identical plots were obtained, which supports the above made assumption that the binuclear complex dissociates in DMF yielding monomeric $[(pydot)CuCl_2(DMF)]$. Corresponding measurements for **P1** and **P2** were carried out in acetone as solvent, again with identical results for both compounds. In CH_2Cl_2 only **P1** could be dissolved and gave also very similar CVs.

All compounds exhibit a reversible and more or less broad reduction wave around 0 V (vs. $FeCp_2/FeCp_2^+$) which is assigned to the Cu^{II}/Cu^{I} redox couple (data in the Supporting Information). Since the reversibility and the shape of the waves depends on the ligands ability to effectively (rapidly) reorganise the ligand sphere after the redox step we can assign the obvious difference between the hexa-coordinate complex (very broad wave) and the other samples (narrow waves) to the rather rigid hexa-coordination (compressed octahedral) and the more flexible $[(O,N,O)CuCl_2(DMF)]$

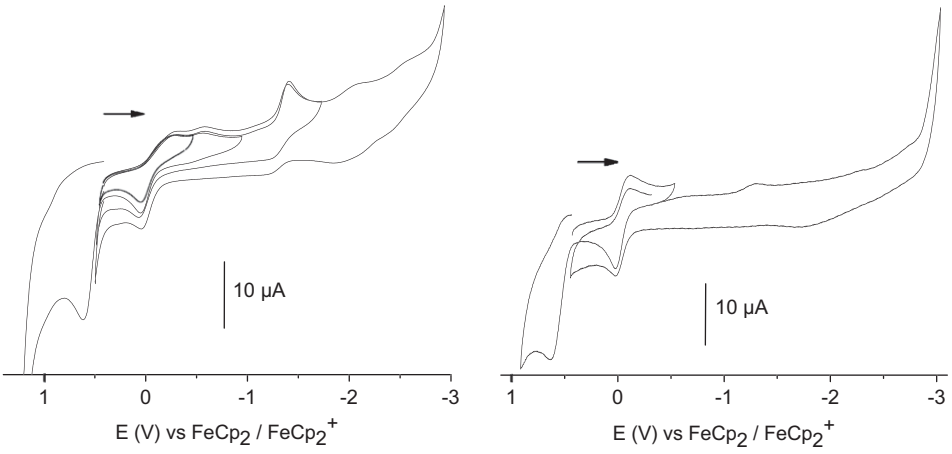

Fig. 4. Cyclic voltammogramms of $[(pydipH_2)_2Cu]Cl_2$ (left) and $[(pydotH_2)CuCl_2]$, measured in DMF/$n Bu_4PF_6$ at 298 K and 100 mV/s scan rate.

coordination. Moreover, in the CV of $[Cu(pydipH_2)_2]^{2+}$ further reduction waves (missing for **P1**) point to partly decomposition (presumably de-coordination of the O,N,O ligand and replacement by DMF). Oxidation waves at about 0.6 V are irreversible in all cases and can be either assigned to further oxidation of copper Cu^{II}/Cu^{III} or more likely to the oxidation of the chloride counter ions or the chlorido ligands $2Cl^-/Cl_2$.

4. Conclusions

The oxido-pincer ligand $pydotH_2$ (2,6-bis(1-hydroxy-1-*o*-tolyl-ethyl-η^2O,O′)pyridine) forms two different Cu^{II} containing complexes when prepared from anhydrous $CuCl_2$. A combination of EPR spectroscopy and EXAFS allowed to structurally characterise the light-green dimer of the formula $[(pydotH_2)CuCl(\mu\text{-}Cl)_2ClCu(pydotH_2)]$ and the penta-coordinate olive-green monomer $[(pydotH_2)CuCl_2]$. The molecular entities imply that the ligand remains protonated upon coordination. When dissolved in DMF both compounds form a monomeric complex $[(pydotH_2)CuCl_2(DMF)]$ which could be characterised in detail by EPR, UV–Vis/NIR spectroscopy and electrochemical measurements. All assignments were supported by comparing Cu^{II} complexes of the related ligands 2,6-bis(hydroxymethyl)pyridine ($pydimH_2$) and 2,6-Bis(1-hydroxy-1-methyl)pyridine ($pydipH_2$). Furthermore, comparative preparative work using all three ligands has allowed some insight into the formation reactions of the various species $[(O,N,O)CuCl_2]_n$ ($n = 1$ or 2), $[(O,N,O)CuCl_2(solv)]$ or $[Cu(O,N,O)_2][CuCl_4]$ which can be obtained from a 1:1 reaction of the ligands and $CuCl_2$ by controlling the reaction conditions. Since the $pydotH_2$ ligand is chiral, there might be some implication on specific spectroscopic properties as IR-frequencies or catalytic properties. However, the focus of this work lies exclusively on the structure elucidation of the two complexes and none of the applied methods is sensitive to the absolute structure.

Acknowledgments

André Uthe and Andreas O. Schüren (University of Cologne) were acknowledged for EPR measurements. We also would like to thank the "Studienstiftung des Deutschen Volkes" (KB) for financial support.

Appendix A. Supplementary data

Supplementary data associated with this article can be found, in the online version, at doi:10.1016/j.poly.2011.10.023.

References

[1] E.I. Solomon, U.M. Sundaram, T.E. Machonkin, Chem. Rev. 96 (1996) 2563.
[2] (a) I. Bertini, G. Cavallaro, K.S. McGreevy, Coord. Chem. Rev. 254 (2010) 506; (b) A.K. Boal, A.C. Rosenzweig, Chem. Rev. 109 (2009) 4760.
[3] R.H. Holm, P. Kennepohl, E.I. Solomon, Chem. Rev. 96 (1996) 2239.
[4] W. Kaim, J. Rall, Angew. Chem. Int. Ed. Engl. 35 (1996) 43.
[5] B.J. Hathaway, Coord. Chem. Rev. 52 (1983) 87.
[6] V. Chaurin, E.C. Constable, C.E. Housecroft, New J. Chem. 30 (2006) 1740.
[7] W. Kaim, Dalton Trans. (2003) 761.
[8] M.A. Halcrow, Dalton Trans. (2003) 4375.
[9] (a) N. Wei, N.N. Murthy, K.D. Karlin, Inorg. Chem. 33 (1994) 6093; (b) G. Kokoszka, K.D. Karlin, F. Padula, J. Baranowski, C. Goldstein, Inorg. Chem. 23 (1984) 4378.
[10] D. Reinen, C. Friebel, Inorg. Chem. 23 (1984) 791.
[11] R.J.M. Klein Gebbink, R.T. Jonas, C.R. Goldsmith, T.D.P. Stack, Inorg. Chem. 41 (2002) 4633.
[12] F.M. Al-Sogair, B.P. Operschall, A. Sigel, H. Sigel, J. Schnabl, R.K.O. Sigel, Chem. Rev. 111 (2011) 4964.
[13] A.A. El-Sherif, M.M. Shoukry, Spectrochim. Acta A66 (2007) 691.
[14] S. Bhattacharya, K. Snehalatha, S.K. George, J. Org. Chem. 63 (1998) 27.
[15] J.D. Crowley, K.D. Hänni, D.A. Leigh, A.M.Z. Slawin, J. Am. Chem. Soc. 132 (2010) 5309.
[16] A.K. Gupta, J. Kim, Acta Crystallogr C59 (2003) m262.
[17] S. Winter, W. Seichter, E. Weber, Z. Anorg. Allg. Chem. 630 (2004) 434.
[18] M. Koman, M. Melník, T. Glowiak, Cryst. Res. Technol. 37 (2002) 119.
[19] T.C. Stamatatos, G.C. Vlahopoulou, C.P. Raptopoulou, A. Terzis, A. Escuer, S.P. Perlepes, Inorg. Chem. 48 (2009) 4610.
[20] G.C. Vlahopoulou, D.I. Alexandropoulos, C.P. Raptopoulou, S.P. Perlepes, A. Escuer, T.C. Stamatatos, Polyhedron 28 (2009) 3235.
[21] M. Melnik, M. Koman, L. Macaskova, T. Glowiak, R. Grobelny, J. Mrozinsky, J. Coord. Chem. 43 (1998) 159.
[22] (a) V.T. Yilmaz, S. Guney, O. Andac, W.T.A. Harrison, J. Coord. Chem. 56 (2003) 21; (b) O. Andac, S. Guney, Y. Topcu, V.T. Yilmaz, W.T.A. Harrison, Acta Crystallogr. C58 (2002) m17.
[23] (a) M. Melnik, C.E. Holloway, J. Coord. Chem. 49 (1999) 69; (b) M. Koman, M. Melnik, Polyhedron 16 (1997) 2721.
[24] M. Koman, M. Melnik, J. Moncol, Inorg. Chem. Commun. 3 (2000) 262.
[25] A. Klein, S. Elmas, K. Butsch, Eur. J. Inorg. Chem. (2009) 2271.
[26] A. Klein, K. Butsch, J. Neudörfl, Inorg. Chim. Acta 363 (2010) 3282.
[27] S. Autzen, H.-G. Korth, R. Boese, H. de Groot, R. Sustmann, Eur. J. Inorg. Chem. (2003) 1401.
[28] J.E. Weder, C.T. Dillon, T.W. Hambley, B.J. Kennedy, P.A. Lay, J.R. Biffin, H.L. Regtop, N.M. Davies, Coord. Chem. Rev. 232 (2002) 95.
[29] (a) M. Newville, J. Synchrotron. Rad. 8 (2001) 322; (b) B. Ravel, M. Newville, J. Synchrotron. Rad. 12 (2005) 537.
[30] M. Newville, P. Livins, Y. Yacoby, J.J. Rehr, E.A. Stern, Phys. Rev. B 47 (1993) 14126.
[31] N. Binsted, S.S. Hasnain, J. Synchrotron. Rad. 3 (1996) 185.
[32] (a) S. Winter, W. Seichter, E. Weber, J. Coord. Chem. 57 (2004) 997; (b) V.T. Yilmaz, S. Hamamci, C. Thöne, Polyhedron 23 (2004) 841.
[33] (a) P. Kapoor, A. Pathak, P. Kaur, P. Venugopalan, R. Kapoor, Trans. Met. Chem. 29 (2004) 251; (b) P. Kapoor, A. Pathak, R. Kapoor, P. Venugopalan, M. Corbella, M. Rodriguez, J. Robles, A. Llobet, Inorg. Chem. 41 (2002) 6153.
[34] I.A. Koval, M. Sgobba, M. Huisman, M. Lüken, E. Saint-Aman, P. Gamez, B. Krebs, J. Reedijk, Inorg. Chim. Acta 359 (2006) 4071.
[35] C. Lamberti, S. Bordiga, M. Salvalaggio, G. Spoto, A. Zecchina, F. Geobaldo, G. Vlaic, M. Bellatreccia, J. Phys. Chem. B 101 (1997) 344.
[36] (a) L.-S. Kau, D.J. Spira-Solomon, J.E. Penner-Hahn, K.O. Hodgson, E.I. Solomon, J. Am. Chem. Soc. 109 (1987) 6433; (b) C. Lamberti, G. Spoto, D. Scarano, C. Pazé, M. Salvalaggio, S. Bordiga, A. Zecchina, G. Turnes Palomino, F. D'Acapito, Chem. Phys. Lett. 269 (1997) 500.
[37] N. Kosugi, H. Kondoh, H. Tajima, H. Kuroda, Chem. Phys. 135 (1989) 149.
[38] J. Prasad, V. Krishna, H.L. Nigam, J. Chem. Soc., Dalton Trans. (1976) 2413.
[39] S.K. Joshi, B.D. Shrivastava, R.C. Kumawat, K.B. Pandeya, Jpn. J. Appl. Phys. 32 (Suppl. 32–2) (1993) 830.
[40] (a) C.K. Bhaskare, S.Y. Kulkarni, Prog. Indian Acad.Sci. Chem. Sci. 97 (1986) 25; (b) H.L. Nigam, U.C. Srivastava, Chem. Commun. 14 (1971) 761.
[41] T. Glowiak, I. Podgorska, Inorg. Chim. Acta 125 (1986) 83.
[42] (a) W.A. Alves, R.H. de Almeida Santos, A. Paduan-Filho, C.C. Becerra, A.C. Borin, A.M. Da Costa Ferreira, Inorg. Chim. Acta 357 (2004) 2269; (b) W.A. Alves, S.A. de Almeida Filho, R.H. de Almeida Santos, A.M. Da Costa Ferreira, Inorg. Chem. Commun. 6 (2003) 294.
[43] S. Thakurta, P. Roy, G. Rosair, C.J. Gómez-García, E. Garribba, S. Mitra, Polyhedron 28 (2009) 695.
[44] K. Skorda, T.C. Stamatatos, A.P. Vafiadis, A.T. Lithoxoidou, A. Terzis, S.P. Perlepes, J. Mrozinski, C.P. Raptopoulou, J.C. Plakatouras, E.G. Bakalbassis, Inorg. Chim. Acta 358 (2005) 565.
[45] (a) L.J. Singh, N.S. Devi, S.P. Devi, W.B. Devi, R.K.H. Singh, B. Rajeswari, R.M. Kadam, Inorg. Chem. Commun. 13 (2010) 365; (b) P.K. Nanda, M. Bera, A.M. Da Costa Ferreira, A. Paduan-Filho, D. Ray, Polyhedron 28 (2009) 4065; (c) S.P. Devi, R.K.H. Singh, R.M. Kadam, Inorg. Chem. 45 (2006) 2193.
[46] (a) S.K. Hoffmann, D. Towle, W.E. Hatfield, P. Chaudhuri, K. Wieghardt, Inorg. Chem. 24 (1985) 1307; (b) N.F. Albanese, H.M. Haendler, Polyhedron 2 (1983) 1131.
[47] S.S. Eaton, K.M. More, B.M. Sawant, G.R. Eaton, J. Am. Chem. Soc. 105 (1983) 6560.
[48] B.J. Hathaway, D.E. Billing, Coord. Chem. Rev. 5 (1970) 143.